



## Influence of BLT content on phase structure and electrical properties of (1-x)BT-xBLT ceramic

Navavan THONGMEE<sup>1</sup>, Rattiphorn SUMANG<sup>1</sup>, Soodkhet POJPRAPAI<sup>2</sup>, and Thanawat KLAYTAE<sup>1,\*</sup>

<sup>1</sup>Program of Physics, Faculty of Science and Technology, Pibulsongkram Rajabhat University, Phitsanulok, 65000, Thailand

<sup>2</sup>School of ceramic engineering, Institute of Engineering, Suranaree Univeristy of Technology, Nakornratchsima, 30000, Thailand

\*Corresponding author e-mail: kthanawat@psru.ac.th

### Received date:

12 May 2018

### Accepted date:

17 June 2018

### Keywords:

BT-BLT

Ferroelectric properties

Dielectric properties

Hysteresis loop

### Abstract

(1-x)BaTiO<sub>3</sub>-x(Bi<sub>3.25</sub>La<sub>0.75</sub>)Ti<sub>3</sub>O<sub>12</sub>; (1-x)BT-xBLT ceramics with x = 0-0.20 wt.% were prepared by a solid-state reaction method. The BaTiO<sub>3</sub> (BT) and (Bi<sub>3.25</sub>La<sub>0.75</sub>)Ti<sub>3</sub>O<sub>12</sub> (BLT) powders were, respectively, calcined at 1100°C and 750°C for 4 h. The (1-x)BT-xBLT samples were sintered between 1250°C and 1350°C. The structure exhibited a transformation from tetragonal to orthorhombic with increasing in BLT contents. The average grain size increased with increasing BLT contents. The maximum density and relative density about 6.19 ± 0.07 g/cm<sup>3</sup> and 99.3% were obtained for the composition of 0.95BT-0.05BLT. The Curie temperature (*T<sub>c</sub>*) continuously decreased with increase in BLT contents. The dielectric constant showed a broad peak and pronounced dependence on frequency, which implied an existence of the relaxor behavior. The hysteresis parameters such as saturation polarization (*P<sub>s</sub>*~18.06 μC/cm<sup>2</sup>), remanent polarization (*P<sub>r</sub>*~12.64 μC/cm<sup>2</sup>) and coercive field (*E<sub>c</sub>*~11.09 kV/cm) can be improved when BLT content is increased to 0.05 wt.%.

## 1. Introduction

Barium titanate (BaTiO<sub>3</sub>: BT) lead-free ferroelectric is a typical ferroelectric material with a perovskite-type structure (ABO<sub>3</sub>). It has been used in many applications such as multilayer ceramic capacitors, dielectric ceramic capacitors, thermistors, MEMS, FeRAM etc., because of high a permittivity up to 7000 and piezoelectric constant up to 788 pC/N in textured ceramics [1-3]. BT exhibits a good host matrix and various properties like the electrical resistance, dielectric constant and transition temperatures such as can be effectively controlled by doping with proper impurity ions [4-6]. For example, BT-modified with BiFeO<sub>3</sub> ceramics exhibited large dielectric properties with giant-dielectric-like behavior (dielectric constant ~19000 and loss tangent ~1.4) [7]. Ren et al. and Si et al. [8,9] studied BT ceramic with doped Bi(Ti<sub>0.5</sub>Mg<sub>0.5</sub>)O<sub>3</sub> at 0.2 wt.% can improve the dielectric constant and loss tangent, which is reported to possess lower temperature variation in capacitance in high temperature regions. Patel et al. [10] reported that the polycrystalline of Ba<sub>1-x</sub>La<sub>x</sub>[Ti<sub>0.5</sub>(Fe<sub>0.5</sub>Nb<sub>0.5</sub>)<sub>0.5</sub>]<sub>1-x/4</sub>O<sub>3</sub> [BT-LFN] exhibited dielectric constant ~3200 at room temperature and ~10000 at 350°C with increased La content at 6 mol%. Moreover, many

researchers improved the dielectric properties and tunability by doping rare earth elements such as Ba(Ti<sub>1-x</sub>Yb<sub>4x/3</sub>)O<sub>3</sub> [4], BT doped Bi and Yb [11] and BT doped Er and Yb [12]. Most of the studies on BT by doping of elements show details only in improvement of dielectric properties and loss tangent but there are few reports on the ferroelectric properties of BT-modified.

Among the range of ferroelectric materials, bismuth layer-structure of bismuth lanthanum titanate (Bi<sub>3.25</sub>La<sub>0.75</sub>Ti<sub>3</sub>O<sub>12</sub>:BLT) has simultaneously exhibited ferroelectric, piezoelectric and photoelectric properties [13,14]. It exhibits a higher performance for FRAM devices than PbZr<sub>1-x</sub>Ti<sub>x</sub>O<sub>3</sub> (PZT) perovskite and SrBi<sub>2</sub>Ta<sub>2</sub>O<sub>9</sub> (SBT) Bi-layered structures [15] because of its high Curie temperature (675°C) and excellent fatigue endurance [16]. Recently, BLT ceramics have exhibited highly anisotropic ferroelectric, piezoelectric and dielectric properties. Grain-orientated BLT ceramics have broad dielectric constants and loss tangent peaks. This suggests that textured BLT ceramics has relaxor-like behavior. Moreover, BLT has been studied to improve the ferroelectric properties of thin films and multilayered films also [17,18]. BLT thin film fabricated by a pulsed laser deposition method exhibited a fatigue-free characteristic and a large

remnant polarization [17]. When BLT multilayered films were combined with the superior ferroelectric properties of PZT, this can enhance ferroelectric properties [18]. However, PZT contains a toxic element (Pb) which harms the environment [19-23]. Therefore, mixing two excellent materials with the different structure (BT:  $\text{ABO}_3$  and BLT: bismuth-layer structure) has been attempted to improve ferroelectric properties on  $(1-x)\text{BT}-x\text{BLT}$  ceramics and replace PZT. Therefore, the influence of BLT contents on phase structure, microstructure, dielectric and ferroelectric properties of  $(1-x)\text{BT}-x\text{BLT}$  ceramics prepared by solid-state reaction method is the aim of the study.

## 2. Experimental

$(1-x)\text{BaTiO}_3-x(\text{Bi}_{3.25}\text{La}_{0.75})\text{Ti}_3\text{O}_{12}$ ;  $(1-x)\text{BT}-x\text{BLT}$  ceramics with  $x = 0-0.20$  wt.% were prepared by a solid-state reaction method.  $\text{Bi}_2\text{O}_3$  (99.5%),  $\text{BaCO}_3$  (98.0%),  $\text{TiO}_2$  (99.5%) and  $\text{La}_2\text{O}_3$  (99.9%) were chosen as the starting raw materials. These raw materials were weighed according to the stoichiometric formula and ball milled again for 24 h. The mixed powders were subsequently dried and separately calcined at  $1100^\circ\text{C}/4\text{h}$ . for BT and  $750^\circ\text{C}/4\text{h}$ . for BLT. The BT and BLT calcined powders were then weighted and blended according to the formulas of  $(1-x)\text{BT}-x\text{BLT}$ . The calcined powders were pressed into discs of 10 mm in diameter and 1-2 mm in thickness. The green pellets were sintered from  $1100^\circ\text{C}$  to  $1400^\circ\text{C}$  for 4 h in air at heating/cooling rate of  $5^\circ\text{C}/\text{min}$ .

Phase structure of the powders and ceramics were identified using X-ray diffraction (XRD, Philip PW 3040/60 X'Pert Pro). The grain morphology of the samples was observed by means of scanning electron microscopy (SEM, Leol4555VP). The theoretical density for each composition was calculated using the law of mixing and the densities of  $\text{BaTiO}_3$  and  $(\text{Bi}_{3.25}\text{La}_{0.75})\text{Ti}_3\text{O}_{12}$  pure phases, which were  $6.07\text{ g/cm}^3$  (ICSD no. 05-0626) and  $7.67\text{ g/cm}^3$  (ICSD no. 15-0091), respectively. For electrical characterization, samples were polished and painted with silver paste on the surfaces. Dielectric constant and loss of the ceramics for a wide variety of frequencies in the temperature range of  $30^\circ\text{C}$  to  $250^\circ\text{C}$  were measured using an LCR meter (Agilent 4284A). The polarization-electric field ( $P$ - $E$ ) hysteresis loops was measured using the

ferroelectric test system which connected to a high voltage amplifier (Model 20/20C, Trek).

## 3. Result and discussion

The XRD pattern of  $(1-x)\text{BT}-x\text{BLT}$  mixed powders at differences BLT contents are shown in Figure 1 (a). The XRD peaks of pure BT powders match with that reported for  $\text{BaTiO}_3$  with tetragonal structure (ICSD no. 05-0626) and correspond with a previous work [1]. When increasing in BLT contents, the XRD peaks including (117) (0012) (020) (028) (220) (1115) and (317), which are the main pattern of  $\text{Bi}_{3.25}\text{La}_{0.75}\text{Ti}_3\text{O}_{12}$  with orthorhombic phase (ICSD no. 15-0091), are observed at  $2\theta$  range of  $30^\circ - 58^\circ$  [24]. The intensity of these peaks increased with an increase of BLT contents. This can be attributed to the mixed powers coexisting phases between tetragonal and orthorhombic phase with an increase of BLT contents. The XRD patterns of  $(1-x)\text{BT}-x\text{BLT}$  ceramics at differences BLT contents are shown in Figure 1 (b). All the sintered samples show a pure phase, indicating that  $\text{Bi}^{2+}$  and  $\text{La}^{3+}$  ions are incorporated into the perovskite structure. For the pure BT, the phase structure shows the double peaks of  $(002)_\text{T}$  and  $(200)_\text{T}$  at  $2\theta$  around  $45^\circ - 48^\circ$ . When the BLT contents increase, the  $(002)_\text{T}$  and  $(200)_\text{T}$  peak combines and becomes a single  $(0016)_\text{O}$  peak. This indicates a co-existence of tetragonal and orthorhombic phases in the composition with addition of BLT contents. It also indicates that the rise in BLT contents results in the increase of the orthorhombic and the decrease of the tetragonal phases. Moreover, the intensity ratios of  $(200)_\text{T}/(002)_\text{T}$  peaks gradually decrease with increasing BLT contents, indicating the presence of slight lattice distortions.

Figure 2 illustrates the SEM images of  $(1-x)\text{BT}-x\text{BLT}$  ceramics at different BLT contents. The pure BT sample presents irregular morphology shape and small porous microstructure form (Figure 2(a)). The grains exhibit rod-like grain growth and the porosity decreases with an increasing amount of BLT contents ( $x = 0.05$ ) as seen in Figure 2(b). When there was an increase in BLT content ( $x = 0.10$ ), the grain shape changes from the rod-like to a more spherical-like grain and pore size increases. The increased in porosity at the high concentration of BLT content may be due to the volatile alkali metal [25]. The cross-section microstructures of the sintered ceramics are displayed in Figures 2(d)-(f).

The pure BT sample exhibits mixed types of fracture sinter-granular and intra-granular. When BLT contents increases, the sintered ceramic exhibits nearly fully intra-granular fracture (Figure 2(e) and (Figure 2(f)). This is attributed to the addition of BLT contents which makes the grain boundary of ceramic harder. The measured bulk density and relative density of (1-x)BT-xBLT ceramics at different BLT contents is shown in Figure 3. Generally, the density of pure BT is 6.07 g/cm<sup>3</sup> and BLT is 7.67 g/cm<sup>3</sup> (ICSD no. 05-0626 and no. 15-0091). In this study, the bulk density and relative density are between 5.85 ± 0.12 g/cm<sup>3</sup> to

6.19 ± 0.02 g/cm<sup>3</sup> and 96.3% to 99.3%, respectively. For pure BT, the bulk density and relative density are 5.85 ± 0.12 g/cm<sup>3</sup> and 96.3%. With increasing in BLT contents, the bulk density and relative density values increase and show the maximum value of 6.16 ± 0.02 g/cm<sup>3</sup> and 99.3% of relative density at a composition of 0.05 wt.%. For BLT content > 0.05 wt.%, the bulk density and relative density decrease. The decrease in bulk density and relative density may be attributed to the porous microstructure which is revealed by SEM result in Figures 2(c) and (f).

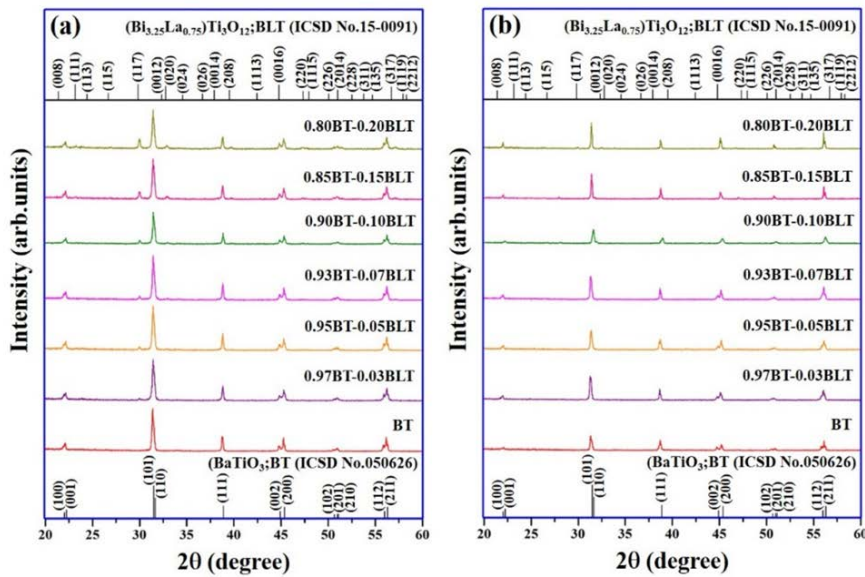


Figure 1. XRD patterns of the (1-x)BT-xBLT (a) calcined powders and (b) sintered ceramics at differences x(BLT) contents.

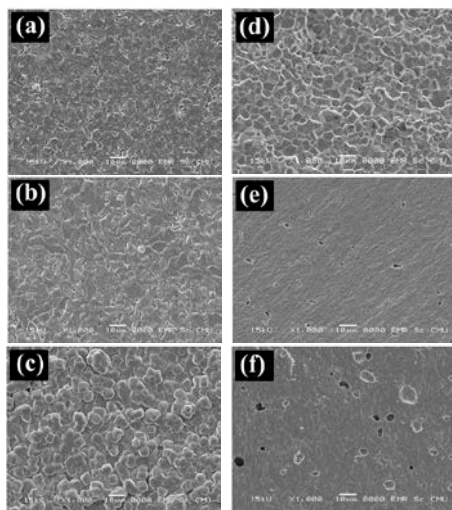


Figure 2. Surface morphologies of (1-x)BT-xBLT ceramics: (a) x(BLT) = 0, (b) x(BLT) = 0.05 and (c) x(BLT) = 0.10 and fracture surface micrographs: (d) x(BLT) = 0, (e) x(BLT) = 0.05 and (f) x(BLT) = 0.10.

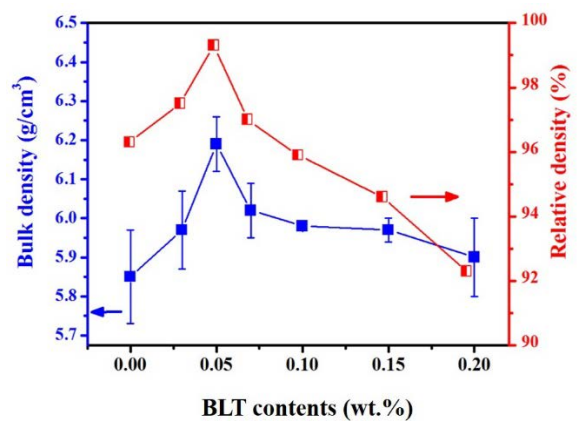


Figure 3. Bulk density and relative density of (1-x)BT-xBLT ceramics at difference x(BLT) contents.

Figure 4 shows the temperature dependence of the dielectric constant ( $\epsilon_r$ ) and loss tangent ( $\tan\delta$ ) of (1-x)BT-xBLT ceramic with various BLT contents as functions of temperature and different frequencies between 1 kHz and 1 MHz. All the samples showed that the dielectric properties changes significantly with temperature. For pure BT ceramics, the maximum values of the dielectric constant are obtained as expected at the Curie temperature ( $T_c$ ) at 134°C, which shows the maximum value of 10250 (Figure 4(a)). Upon increasing the temperature above the Curie temperature,  $\epsilon_r$  decreases to its value at the room temperature. By increasing BLT contents,  $\epsilon_r$  and  $T_c$  decreases from 10250 to 3787 and 134°C to 44°C, respectively (listed in Table 1). The  $T_c$  shifts may be related to the change of a grain size with BLT doping concentration, (see in Table 1) [26]. The loss tangent also decreases and then increases by a small value with doping of BLT contents. Moreover, all of ceramics exhibited broad peaks and an obvious frequency dependence. With increasing frequency,  $T_c$  moves to higher temperature regions. The board  $\epsilon_r$  peak (at  $T_c$ ) and the character of the temperature dependence of  $\epsilon_r$  (at  $T_c$ ) show a typical relaxor characteristic. The diffuseness exponent ( $\gamma$ ) of ceramics increased from 1.15 to 1.57 with an increase in BLT contents (see in Table 1), indicating that the (1-x)BT-xBLT solid solutions show diffuse phase transition behaviour. These results may imply a presence of the relaxor feature.

The ferroelectric properties of (1-x)BT-xBLT ceramics are characterized by the  $P$ - $E$  hysteresis loops showed in Figure. 5. For pure the BT samples, the hysteresis loop is not well saturated ( $P_s = 22.1 \mu\text{C}/\text{cm}^2$ ,  $P_r = 8.6 \mu\text{C}/\text{cm}^2$  and  $E_c = 5.6 \text{ kV}/\text{cm}$ ) (see Figure 5(a)). The ferroelectric properties are similar with the result of Deshpande et al. [1] who have reported the  $P_s = 13.0 \mu\text{C}/\text{cm}^2$ ,  $P_r = 7.0 \mu\text{C}/\text{cm}^2$  and  $E_c = 4.0 \text{ kV}/\text{cm}$ . Sharma et al. [27] have reported that the  $P_s = 19.2 \mu\text{C}/\text{cm}^2$ ,  $P_r = 11.1 \mu\text{C}/\text{cm}^2$  and  $E_c = 8.0 \text{ kV}/\text{cm}$  for the sol-gel derived BT ceramics. By increasing in BLT contents up to 0.05 wt.%, the  $P$ - $E$  hysteresis loops become more saturated with the  $P_s$  slightly decreasing from 22.1  $\mu\text{C}/\text{cm}^2$  to 18.06  $\mu\text{C}/\text{cm}^2$  while  $P_r$  tending to increase from 8.6  $\mu\text{C}/\text{cm}^2$  to 12.64  $\mu\text{C}/\text{cm}^2$ . At BLT = 0.05 wt.% and BLT = 0.07 wt.%, these samples exhibit unsaturated ferroelectric loops and the existence of the large leakage current with applied electric field [28]. This is related with the higher level of porosity and loss tangent which can be confirmed by the results of SEM and dielectric measurement, respectively. At BLT > 0.10 wt.%, the sample exhibits a slim  $P$ - $E$  hysteresis loop, which is

consistent with a relaxor behaviour on introducing BLT contents. The value of  $P_s$  and  $P_r$  are 9.76  $\mu\text{C}/\text{cm}^2$  and 3.96  $\mu\text{C}/\text{cm}^2$  for BLT = 0.15 wt.% and 6.93  $\mu\text{C}/\text{cm}^2$  and 0.73  $\mu\text{C}/\text{cm}^2$  for BLT = 0.20 wt.% (listed in Table 1). An increasing  $P_s$  and  $P_r$  with BLT = 0.05 wt.% and BLT = 0.07 wt.% may be attributed to the increase of grain size, low porosity and the site occupancy of ions. An increase in grain size affects electrical properties because ferroelectric domains are easy to stabilize; this was found in many systems such as BT-LFN [10], BT and PLZT ceramics [29] and BLT [30]. Another factor may be contributed to the  $\text{La}^{3+}$  and  $\text{Ba}^{2+}$  ions occupied A-sites favoring the formation of donor imperfections in (1-x)BT-xBLT ceramics. However, these ions may also occupy the B-sites for higher composition of BLT contents which represent acceptors.  $V_O^{\bullet\bullet}$  and  $V_{B-site}^{\bullet\bullet}$  may form dipoles according to Coulomb's law of attraction [15]. Therefore, these compositions present the high values of  $P_s$  and  $P_r$ . A decreasing  $P_s$  and  $P_r$  at BLT > 0.07 wt.% with larger grains is because of the higher degree of the porous microstructure and the lower concentration of grain boundaries.

#### 4. Conclusions

(1-x)BaTiO<sub>3</sub>-x(Bi<sub>3.25</sub>La<sub>0.75</sub>)Ti<sub>3</sub>O<sub>12</sub>; (1-x)BT-xBLT ceramics with  $x = 0$ -0.20 wt.% were successfully prepared by a solid-state reaction method. The BLT contents affects phase formation, microstructure and electrical properties of (1-x)BT-xBLT ceramics. The sintered ceramics show a pure phase, indicating that  $\text{Bi}^{2+}$  and  $\text{La}^{3+}$  ions are incorporated into the perovskite structure. The cross-section microstructures show both mixed sinter-granular and intra-granular fracture surfaces for pure BT and change to nearly fully intra-granular fracture for the sample with added BLT contents. The bulk density and relative density increase first and then drop with the increasing of BLT contents.  $\epsilon_r$  and  $T_c$  decrease from 10250 to 3787 and 134°C to 44°C, respectively, with an increase in BLT contents. The ceramic samples exhibit board  $\epsilon_r$  peaks and the temperature dependence;  $\epsilon_r$  shows a typical relaxor characteristic. The  $P$ - $E$  hysteresis loop becomes more saturated with increasing in BLT contents. At the high concentration of BLT content, the ceramics showed the existence of the large leakage current with the applied electric field due to the higher degree of porosity and dielectric loss. The maximum value of density, relative density,  $P_s$  and  $P_r$  are  $6.19 \pm 0.07 \text{ g}/\text{cm}^3$ , 99.3%, ~18.06  $\mu\text{C}/\text{cm}^2$  and ~12.64  $\mu\text{C}/\text{cm}^2$ , respectively, in the composition 0.95BT - 0.05BLT.

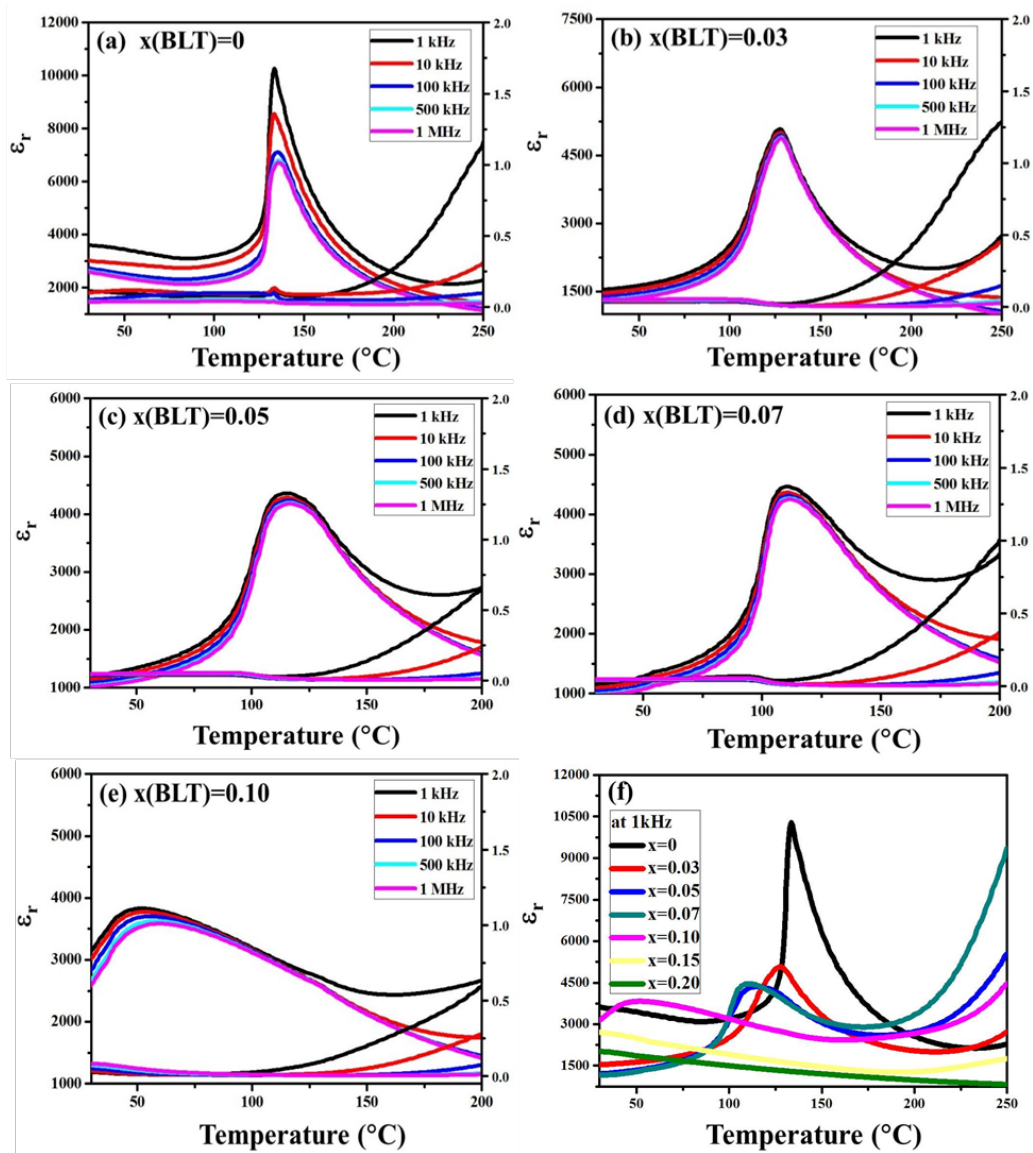


**Figure 4.** Dielectric properties of (1-x)BT-xBLT ceramics at differences frequency: (a)  $x(\text{BLT}) = 0$ , (b)  $x(\text{BLT}) = 0.03$ , (c)  $x(\text{BLT}) = 0.05$ , (d)  $x(\text{BLT}) = 0.07$ , (e)  $x(\text{BLT}) = 0.10$  and (f) differences of  $x(\text{BLT})$  contents.

**Table 1.** Average grain size, bulk density, relative density,  $\epsilon_r$ ,  $\tan\delta$ ,  $\gamma$ ,  $T_c$ ,  $P_r$ ,  $P_s$  and  $E_c$  of (1-x)BT-xBLT ceramics at difference of  $x(\text{BLT})$  contents.

Compositions	Average grain size ( $\mu\text{m}$ )	Bulk density ( $\text{g}/\text{cm}^3$ )	Relative density (%)	$\epsilon_r$	$\tan\delta$	$\gamma$	$T_c$ ( $^{\circ}\text{C}$ )	$P_r$ ( $\mu\text{C}/\text{cm}^2$ )	$P_s$ ( $\mu\text{C}/\text{cm}^2$ )	$E_c$ (kV/cm)
$x(\text{BLT}) = 0$	$0.74 \pm 0.23$	$5.85 \pm 0.12$	96.3	10250	0.10	1.15	134	8.60	22.14	5.68
$x(\text{BLT}) = 0.03$	$2.16 \pm 2.16$	$5.97 \pm 0.10$	97.5	5065	0.02	1.32	128	9.63	17.85	8.26
$x(\text{BLT}) = 0.05$	$3.13 \pm 1.47$	$6.19 \pm 0.07$	99.3	4367	0.02	1.48	114	12.64	18.06	11.09
$x(\text{BLT}) = 0.07$	$4.21 \pm 0.64$	$6.02 \pm 0.07$	97.0	4477	0.03	1.53	110	18.40	18.90	12.68
$x(\text{BLT}) = 0.10$	$5.27 \pm 1.61$	$5.98 \pm 0.01$	95.9	3787	0.03	1.57	44	10.79	17.27	9.80
$x(\text{BLT}) = 0.15$	$5.60 \pm 0.92$	$5.97 \pm 0.03$	94.6	-	-	-	-	3.96	9.76	11.24
$x(\text{BLT}) = 0.20$	$7.71 \pm 1.81$	$5.90 \pm 0.10$	92.3	-	-	-	-	0.73	6.93	0.68

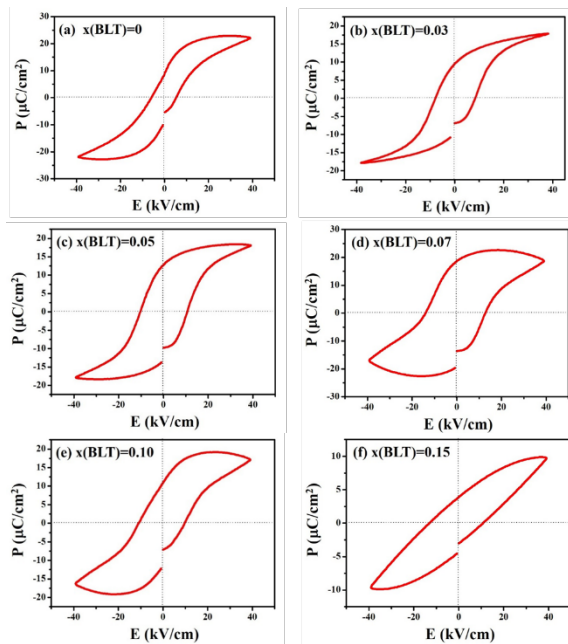


**Figure 5.** Ferroelectric properties of  $(1-x)\text{BT}-x\text{BLT}$  ceramics recorded at room temperature: (a)  $x(\text{BLT}) = 0$ , (b)  $x(\text{BLT}) = 0.03$ , (c)  $x(\text{BLT}) = 0.05$ , (d)  $x(\text{BLT}) = 0.07$ , (e)  $x(\text{BLT}) = 0.10$  and (f)  $x(\text{BLT}) = 0.15$ .

## 5. Acknowledgements

This work financially supported by the National Research Council of Thailand (NRCT) through Pibulsongkram Rajabhat University (Grant no. RDI-160-6-7). Thanks are given to Dr. Nitish Kumar for his help in editing the manuscript.

## References

- [1] S. B. Deshpande, P. D. Godbole, Y. B. Kholam, and H. S. Potdar, "Characterization of barium titanate:  $\text{BaTiO}_3$  (BT) ceramics prepared from sol-gel derived BT powders," *Journal of Electroceramics*, vol. 15, pp. 103–108, 2005.
- [2] T. Ramoška, J. Banys, R. Sobiestianskas, M. Vijatović Petrović, J. Bobić, and B. Stojanović, "Dielectric investigations of La-doped barium titanate," *Processing and Application of Ceramics*, vol. 4, pp. 193–198, 2010.
- [3] J. Zhu, C. Jin, W. Cao, and X. Wang, "Phase transition and dielectric properties of nanograin  $\text{BaTiO}_3$  ceramic under high pressure," *Applied Physics Letters*, vol. 92, pp. 1–3, 2008.
- [4] M. Ganguly, S. K. Rout, C. W. Ahn, I. W. Kim, and K. Manoranjan, "Structural, electrical and optical properties of  $\text{Ba}(\text{Ti}_{1-x}\text{Yb}_{4x/3})\text{O}_3$  ceramics," *Ceramics International*, vol. 39, pp. 9511–9524, 2013.
- [5] S. Garcia, R. Font, J. Portelles, R. J. Quinones, J. Heiras, and J. M. Siqueiros, "Effect of Nb doping on  $(\text{Sr},\text{Ba})\text{TiO}_3$  (BST) ceramic samples," *Journal of Electroceramics*, vol. 6, pp. 101–108, 2001.
- [6] M. Aparna, T. Bhimasankaram, S. V. Suryanarayanan, G. Prasad, and G. S. Kumar, "Effect of lanthanum doping on electrical and electromechanical properties of  $\text{BaTiO}_3$ ," *Bulletin of Materials Science*, vol. 24, pp. 497–504, 2001.
- [7] S. Chandarak, A. Ngamjarrojana, S. Srilomsak, P. Laoratanakul, S. Rujirawat, and R. Yimnirun, "Dielectric Properties of  $\text{BaTiO}_3$ -Modified  $\text{BiFeO}_3$  Ceramics," *Ferroelectrics*, vol. 410, pp. 75–81, 2011.
- [8] P. Ren, X. Wang, H. Fan, Y. Ren, and G. Zhao, "Structure, relaxation behaviours and nonlinear dielectric properties of  $\text{BaTiO}_3$ - $\text{Bi}(\text{Ti}_{0.5}\text{Mg}_{0.5})\text{O}_3$  ceramics," *Ceramics International*, vol. 41, pp. 7693–7697, 2015.
- [9] F. Si, T. Bin, Z. Fang, and S. Zhang, "Nb-doped  $0.8\text{BaTiO}_3$ - $0.2\text{Bi}(\text{Mg}_{0.5}\text{Ti}_{0.5})\text{O}_3$  ceramics with stable dielectric properties at high temperature," *Crystals*, vol. 7, pp. 168, 2017.
- [10] P. K. Patel, J. Rani, N. Adhlakha, H. Singh, and K. L. Yadav, "Enhanced dielectric properties of doped barium titanate ceramics," *Journal of Physics and Chemistry of Solids*, vol. 74, pp. 545–549, 2013.
- [11] G. Yao, X. Wang, Y. Yang, and L. Li, "Effects of  $\text{Bi}_2\text{O}_3$  and  $\text{Yb}_2\text{O}_3$  on the Curie temperature in  $\text{BaTiO}_3$ -based ceramics," *Journal of the American Ceramic Society*, vol. 93, pp. 1697–1701, 2010.
- [12] A. G. Murillo, F. J. C. Romo, M. G. Hernandez, J. R. Salgado, M. A. D. Crespo, S. A. P. Sanchez, and H. Terrones, "Structural and morphological characteristics of polycrystalline  $\text{BaTiO}_3$ :  $\text{Er}^{3+}$ ,  $\text{Yb}^{3+}$  ceramics synthesized by the sol-gel route: influence of chelating agents," *Journal of Sol-Gel Science and Technology*, vol. 53, pp. 121–133, 2010.
- [13] J. Y. Han, and C. W. Bark. "Influence of calcination temperature on the structure and optical properties of  $\text{Bi}_{3.25}\text{La}_{0.75}\text{Ti}_3\text{O}_{12}$  powders," *Journal of the Korean Physical Society*, vol. 65, pp. 216–221, 2014.
- [14] J. Liu, and Z. Shen, "Dielectric, piezoelectric, and ferroelectric properties of grain-

- orientated  $\text{Bi}_{3.25}\text{La}_{0.75}\text{Ti}_3\text{O}_{12}$  ceramics,” *Journal of Applied Physics*, vol. 102, pp. 104–107, 2007.
- [15] S. Ma, X. Cheng, J. Hao, W. Li, R. Chu, and Z. Xu, “Dielectric and ferroelectric properties of Ta-modified  $\text{Bi}_{3.25}\text{La}_{0.75}\text{Ti}_3\text{O}_{12}$  ceramics,” *Ceramics International*, vol. 43, pp. 13193–13198, 2017.
- [16] J. H. Park, J. S. Bae, B. C. Choi, and J. H. Jeong, “Impedance spectroscopy of  $\text{Bi}_{3.25}\text{La}_{0.75}\text{Ti}_3\text{O}_{12}$  ceramics above and below ferroelectric transition temperatures,” *Journal of Physics D: Applied Physics*, vol. 40, pp. 579–583, 2007.
- [17] J. H. Park, J. S. Bae, B. C. Choi, and J. H. Jeong, “Effect of Nb doping of ferroelectric properties of  $\text{Bi}_{3.25}\text{La}_{0.75}\text{Ti}_3\text{O}_{12}$  ceramics,” *Journal of Applied Physics*, vol. 97, pp. 064110, 2005.
- [18] J. Li, P. Li, G. Zhang, J. Yu, Y. Wu, and X. Wen, “The thickness effect of  $\text{Bi}_{3.25}\text{La}_{0.75}\text{Ti}_3\text{O}_{12}$  buffer layer in  $\text{PbZr}_{0.58}\text{Ti}_{0.42}\text{O}_3/\text{Bi}_{3.25}\text{La}_{0.75}\text{Ti}_3\text{O}_{12}$  (PZT/BLT) multilayered ferroelectric thin films,” *Thin Solid Films*, vol. 519, pp. 6021–6025, 2011.
- [19] H. Xinyou, G. Chunhua, C. Xhigang, and L. Huiping, “Influence of composition on properties of BNT-BT lead-free piezoceramics,” *Journal of Rare Earths*, vol. 24, pp. 321–324, 2006.
- [20] J. Li, F. Wang, C. M. Leung, S. W. Or, Y. Tang, X. Chen, T. Wang, X. Qin, and W. Shi, “Large strain response in acceptor- and donor-doped  $\text{Bi}_{0.5}\text{Na}_{0.5}\text{TiO}_3$ -based lead-free ceramics,” *Journal of Materials Science*, vol. 46, pp. 5702–5708, 2011.
- [21] R. Sumang, T. Bongkarn, N. Kumar, and M. Kamnony, “Investigation of a new lead-free  $(1-x-y)\text{BNT}-x\text{BKT}-y\text{BZT}$  piezoelectric ceramics,” *Ceramics International*, vol. 43, pp. 102–109, 2017.
- [22] B. Jaffe, W. R. Cook, and H. Jaffe, *Piezoelectric Ceramics*, London: Academic Press, 1971.
- [23] M. Cernea, G. Poli, G. V. Aldica, C. Berbecaru, B. S. Vasile, and C. Galassi, “Preparation and properties of nanocrystalline BNT-BT  $x$  piezoelectric ceramics by sol-gel and spark plasma sintering,” *Current Applied Physics*, vol. 12, pp. 1100–1105, 2012.
- [24] J. Y. Han, and C. W. Bark, “Tunable band gap of iron-doped lanthanum-modified bismuth titanate synthesized by using the thermal decomposition of a secondary phase,” *Journal of the Korean Physical*, vol. 66, pp. 1371–1375, 2015.
- [25] E. Mostafavi, and A. Ataie, “Fabrication and characterization of nanostructured Ba-doped  $\text{BiFeO}_3$  porous ceramics,” *Materials Science-Poland*, vol. 34, pp. 148–156, 2016.
- [26] Y. Tan, J. Zhang, Y. Wu, C. Wang, V. Koval, B. Shi, H. Ye, R. McKinnon, G. Viola, and H. Yan, “Unfolding grain size effects in barium titanate ferroelectric ceramics,” *Scientific Reports*, vol. 5, pp. 1–9, 2015.
- [27] H. B. Sharma, R. P. Tandon, A. Mansingh, and R. Rup. “Dielectric and piezoelectric properties of sol-gel-derived barium titanate ceramics,” *Journal of Materials Science Letters*, vol. 12, pp. 1795–1796, 1993.
- [28] E. Mostafavi, A. Ataie, M. Ahmadzadeh, M. Palizdar, T. P. Comyn, and A. J. Bell, “Synthesis of nano-structured  $\text{Bi}_{1-x}\text{Ba}_x\text{FeO}_3$  ceramics with enhanced magnetic and electrical properties,” *Materials Chemistry and Physics*, vol. 163, pp. 106–112, 2015.
- [29] H. Maiwa, “Electrocaloric Properties of  $(\text{Pb,L a})(\text{Zr,T i})\text{O}_3$  and  $\text{BaTiO}_3$  Ceramics,” in *Advanced Ceramic Processing*, A. M. A. Mohamed, Eds., United Kingdom: IntechOpen, 2015, pp. 139–150.
- [30] W. Yunyi, Y. Jun, Z. Duanming, Z. Chaodan, Y. Bin, and W. Yunbo, “Effect of bismuth excess on the crystallization of  $\text{Bi}_{3.25}\text{La}_{0.75}\text{Ti}_3\text{O}_{12}$  ceramic and thin Film,” *Integrated Ferroelectrics*, vol. 98, pp. 11–25, 2008.